Renormalization of the soft-quark function and the radiative jet function

Xiang-Peng Wang

G. T. Bodwin, J. Ee and J. Lee: PRD 104 (2021) 1, 016010 & 11, 116025

Power Expansions on the Lightcone Workshop, MITP, Mainz

20^{th} September 2022

Outlines

Introduction: End-point singularity

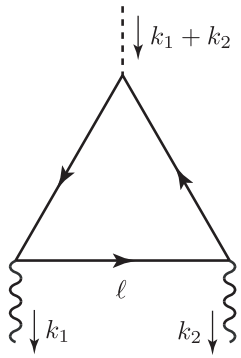

Figure: $H \to b\bar{b} \to \gamma\gamma$ at leading order.

- Large logarithms $\ln(\frac{m_H^2}{m_b^2})$: need resummation
- Traditional light-cone approach leads to end-point divergence $\int_0^1 \frac{1}{z}$, when ℓ becomes soft, $z \to 0$ (z is the fraction of collinear momentum carried by ℓ)
- Generally appears in next-to-leading power corrections

Introduction: Factorization using SCET

Factorization using SCET (Z. L. Liu and M. Neubert, JHEP **04**, 033 (2020) and series of papers):

$$\mathcal{M}_b(H\to\gamma\gamma)=\sum_{i=1}^{3}H_i\langle\gamma\gamma|\mathcal{O}_i|H\rangle, \tag{1}$$

Soft sector (end-point singularities are involved):

$$\begin{aligned}\mathcal{O}_3 \quad &= H(0)\int d^Dx\int d^Dy\,T\Big\{\Big[\Big(\mathcal{A}^{\perp}_{n_1}(x)+\mathcal{G}^{\perp}_{n_1}(x)\Big)\mathcal{X}_{n_1}(x)\Big]^{\alpha i}\bar{\mathcal{X}}^{\beta j}_{n_1}(0)\Big\}\\ &\times T\Big\{\mathcal{X}^{\beta k}_{n_2}(0)\Big[\bar{\mathcal{X}}_{n_2}(y)\Big(\mathcal{A}^{\perp}_{n_2}(y)+\mathcal{G}^{\perp}_{n_2}(y)\Big)\Big]^{\gamma l}\Big\}\\ &\times T\Big\{\Big[S^{\dagger}_{n_2}(y_+)q_s(y_+)\Big]^{\gamma l}\Big[\bar{q}_s(x_-)S_{n_1}(x_-)\Big]^{\alpha i}\Big[S^{\dagger}_{n_1}(0)S_{n_2}(0)\Big]^{jk}\Big\}+\text{h.c.}.\end{aligned} \tag{2}$$

Factorize into convolution of jet functions and soft-quark function ($\omega=\ell_+\ell_-$):

$$\langle\gamma\gamma|\mathcal{O}_3|H\rangle=2g^{\mu\nu}_{\perp}\int_0^{\infty}\frac{d\omega}{\omega}S_1(\omega)\int_{\sqrt{\omega}}^{\infty}\frac{d\ell_-}{\ell_-}J(m_H\omega/\ell_-)J(-m_H\ell_-). \tag{3}$$

Key observations for the non-local renormalization

- The renormalization/evolution kernel of both soft and radiative jet functions are needed to resum logarithms of m_H^2/m_b^2.
- It was not known how to compute the renormalization/evolution of the soft-quark function. We devised a way to do this [G.T Bodwin, J.-H. Ee, J. Lee, X.-P. Wang, PRD 104 (2021) 1, 016010].
- Ze Long Liu and Matthias Neubert JHEP 2020 (2020) 50: "It is an embarrassment that there is no known method in SCET to derive the anomalous dimensions of the jet functions directly from their operator definitions." We solved this problem [G.T Bodwin, J.-H. Ee, J. Lee, X.-P. Wang, arXiv:2107.07941].
- Key observation 1: We should use the unknown all-orders shifted soft-quark funcions or jet functions to replaced the LO ones while extracting the non-local divergences.
- Key observation 2: The radiative jet function contains soft contributions that double-count those in the soft-quark function. One should use in the factorization theorems a subtracted radiative jet function, from which soft contributions have been removed.

Definition of soft function

Soft function:

$$\boldsymbol{S}(\ell_+,\ell_-) = \frac{i\pi}{N_c}\int dx_- dy_+ \exp\left[i\frac{\ell_- y_+ - \ell_+ x_-}{2}\right]$$
$$\times\langle 0|T\,\mathrm{Tr}\Big[S_{n_2}(0)S^\dagger_{n_2}(y_+,0,\mathbf{0}_\perp)q_s(y_+,0,\mathbf{0}_\perp)\bar{q}_s(0,x_-,\mathbf{0}_\perp)S_{n_1}(0,x_-,\mathbf{0}_\perp)S^\dagger_{n_1}(0)\Big]|0\rangle. \tag{4}$$

The momenta flow into the positions x_- and y_+ are fixed by ℓ_+ and ℓ_- respectively, which is required to factorize the two jet functions from the soft-quark function.

It is much easier to do renormalization before integrating $\ell_\perp$ and extracting discontinuity, which does not introduce extra divergences. So we define the un-integrated soft-function:

$$\begin{aligned}\boldsymbol{S}(\ell_+,\ell_-,\ell_\perp) &= \frac{i\pi}{N_c}\int dx_- dy_+ d^{D-2}\boldsymbol{z}_\perp \exp\left[i\left(\frac{\ell_- y_+ - \ell_+ x_-}{2} - \boldsymbol{\ell}_\perp\cdot\boldsymbol{z}_\perp\right)\right]\\ &\times\langle 0|T\,\mathrm{Tr}\Big[S_{n_2}(0,0,\boldsymbol{z}_\perp/2)S^\dagger_{n_2}(y_+,0,\boldsymbol{z}_\perp/2)q_s(y_+,0,\boldsymbol{z}_\perp/2)\\ &\times\bar{q}_s(0,x_-,-\boldsymbol{z}_\perp/2)S_{n_1}(0,x_-,-\boldsymbol{z}_\perp/2)S^\dagger_{n_1}(0,0,-\boldsymbol{z}_\perp/2)\Big]|0\rangle. \end{aligned}\tag{5}$$

Diagrammatic form of $\boldsymbol{S}(\ell_+, \ell_-)$

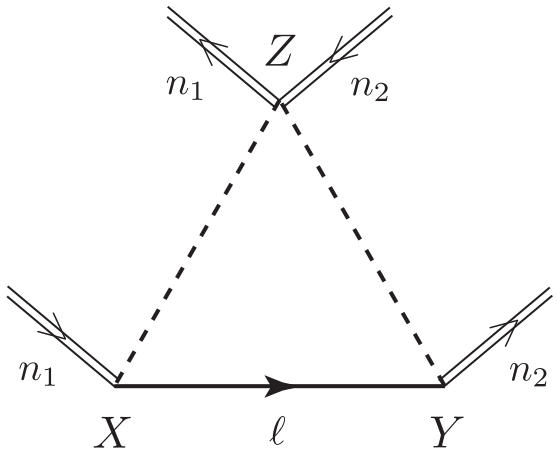

Figure: The solid line is a soft-quark propagator. The double solid lines with incoming arrows are Wilson lines S_{n_i}, and the double solid lines with outgoing arrows are hermitian-conjugate Wilson lines $S_{n_i}^\dagger$. The dashed lines indicate a space-time separation (space-time separations of the jet functions). A jet in the $\pm$ light-front direction is insensitive to external momenta in the $\pm$ or $\perp$ directions, which allows factorization of the Wilson lines of the soft function from the jet functions.

Structure functions and discontinuities

Due to reparameterization invariance, we can decompose the un-integrated soft function into 8 independent structure functions

$$\begin{aligned} \boldsymbol{S}(\ell_+,\ell_-,\ell_\perp) &= m_b \boldsymbol{S}_1(\omega,\boldsymbol{\ell}_\perp^2) + \frac{\not{n}_1}{2}(n_2\cdot\ell)\boldsymbol{S}_2(\omega,\boldsymbol{\ell}_\perp^2) + \frac{\not{n}_2}{2}(n_1\cdot\ell)\boldsymbol{S}_3(\omega,\boldsymbol{\ell}_\perp^2) \\ &\quad + m_b\frac{\not{n}_2\not{n}_1}{4}\boldsymbol{S}_4(\omega,\boldsymbol{\ell}_\perp^2) + \boldsymbol{\ell}_\perp \boldsymbol{S}_5(\omega,\boldsymbol{\ell}_\perp^2) + \frac{m_b\not{n}_1\boldsymbol{\ell}_\perp}{2(n_1\cdot\ell)}\boldsymbol{S}_6(\omega,\boldsymbol{\ell}_\perp^2) \\ &\quad + \frac{m_b\boldsymbol{\ell}_\perp\not{n}_2}{2(n_2\cdot\ell)}\boldsymbol{S}_7(\omega,\boldsymbol{\ell}_\perp^2) + \frac{\not{n}_2\boldsymbol{\ell}_\perp\not{n}_1}{4}\boldsymbol{S}_8(\omega,\boldsymbol{\ell}_\perp^2). \end{aligned} \tag{6}$$

Decomposition of soft function into structure functions

$$\boldsymbol{S}(\ell_+,\ell_-) = m_b\boldsymbol{S}_1(\omega) + \frac{\not{n}_1}{2}(n_2\cdot\ell)\boldsymbol{S}_2(\omega) + \frac{\not{n}_2}{2}(n_1\cdot\ell)\boldsymbol{S}_3(\omega) + m_b\frac{\not{n}_2\not{n}_1}{4}\boldsymbol{S}_4(\omega). \tag{7}$$

Discontinuity of the soft function

$$S_i(\omega) = \frac{1}{2\pi i}[\boldsymbol{S}_i(\omega+i\varepsilon) - \boldsymbol{S}_i(\omega-i\varepsilon)]. \tag{8}$$

Leading-order soft function and discontinuities

Leading-order soft function

$$\boldsymbol{S}^{\rm LO}(\ell_+,\ell_-) \quad = \quad m_b \boldsymbol{S}_1^{\rm LO}(\omega) + \frac{\not{n}_1}{2}\, n_2\cdot\ell\, \boldsymbol{S}_2^{\rm LO}(\omega) + \frac{\not{n}_2}{2}\, n_1\cdot\ell\, \boldsymbol{S}_3^{\rm LO}(\omega), \tag{9}$$

where the LO structure functions are (ϵ poles come from $\ell_\perp$ integration)

$$\boldsymbol{S}_{1,2,3}^{\rm LO}(\omega) \quad = \quad (4\pi)^\epsilon \Gamma(\epsilon) \left(-\omega + m_b^2 - i\varepsilon\right)^{-\epsilon}. \tag{10}$$

The discontinuities of the LO soft structure functions are

$$S_{1,2,3}^{\rm LO}(\omega) \quad = \quad \frac{(4\pi)^\epsilon}{\Gamma(1-\epsilon)} \left(\omega - m_b^2\right)^{-\epsilon} \theta(\omega - m_b^2) = \theta(\omega - m_b^2)\left[1 + O(\epsilon)\right], \tag{11}$$

from which we can see the discontinuities of the LO soft function has no ϵ pole from the $\ell_\perp$ integration.

Difficulties in renormalization of the soft function

The α_s-order soft function is given by Z. L. Liu and M. Neubert, JHEP **04**, 033 (2020), from which one can extract the UV divergences:

$$S^{\rm UV} = \frac{\alpha_s C_F}{4\pi}\left\{\left(\frac{\omega-m_b^2}{\mu^2}\right)^{-2\epsilon}\left[-\frac{2}{\epsilon^2}+\frac{6}{\epsilon}+\frac{2}{\epsilon}\log\left(\frac{\omega-m_b^2}{\omega}\right)\right]\theta(\omega-m_b^2) - \frac{4}{\epsilon}\log\left(\frac{m_b^2-\omega}{m_b^2}\right)\theta(m_b^2-\omega)\right\}. \tag{12}$$

However, the conjectured renormalization factor Z_S given in Z. L. Liu, B. Mecaj, M. Neubert, X. Wang and S. Fleming, JHEP **07**, 104 (2020) is

$$Z_S = \delta(\omega'-\omega)+\frac{\alpha_s C_F}{4\pi}\frac{1}{\epsilon}\left\{\left[\frac{2}{\epsilon}+2\log\left(\frac{\mu^2}{\omega}\right)-3\right]\delta(\omega'-\omega) -4\omega\left[\frac{\theta(\omega'-\omega)}{\omega'(\omega'-\omega)}+\frac{\theta(\omega-\omega')}{\omega(\omega-\omega')}\right]_+\right\}. \tag{13}$$

- The unorthodox momentum routing in the soft function leads to nonlocal contributions in the renormalization
- Explicit fix-order calculation loses the non-local information of the soft function

Renormalization formula

Renormalization of the soft operator $\mathcal{O}_S(\ell_+,\ell_-)$:

$$\mathcal{O}_S^R(\ell_+,\ell_-)=\frac{1}{2}\int d\ell'_+ d\ell'_- Z_S(\ell_+,\ell_-,\ell'_+,\ell'_-;\mu^2)\mathcal{O}_S(\ell'_+,\ell'_-), \quad (14)$$

$$Z_S=Z_S^{(0)}+\alpha_s Z_S^{(1)}+\alpha_s^2 Z_S^{(2)}+\cdots. \quad (15)$$

In terms of vacuum-to-vacuum matrix element,

$$\boldsymbol{S}_i^R(\ell_+,\ell_-)=\frac{1}{2}\int d\ell'_+ d\ell'_- Z_S^{ij}(\ell_+,\ell_-,\ell'_+,\ell'_-;\mu^2)\boldsymbol{S}_j(\ell'_+,\ell'_-), \quad (16)$$

where $\boldsymbol{S}(\ell'_+,\ell'_-)$ is the all-order soft function with shifted arguments.

One-loop UV divergent diagrams

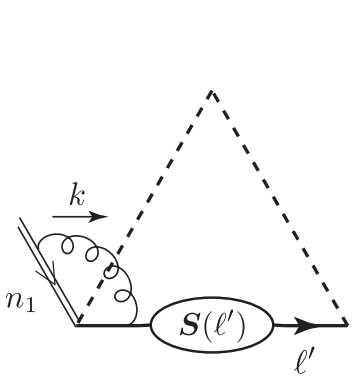

$\ell' = (\ell_+, \ell_-, \boldsymbol{\ell}_\perp)$

(a)

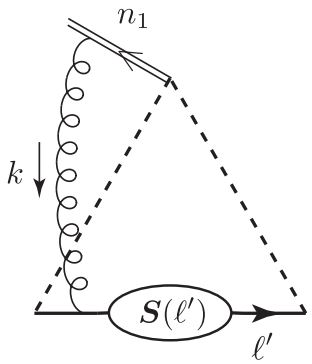

$\ell' = (\ell_+ + k_+, \ell_-, \boldsymbol{\ell}_\perp)$

(b)

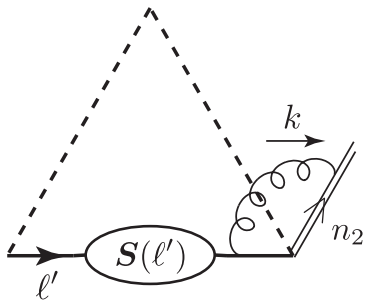

$\ell' = (\ell_+, \ell_-, \boldsymbol{\ell}_\perp)$

(a)

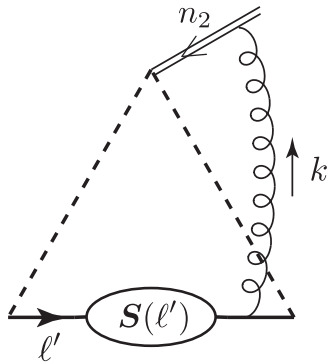

$\ell' = (\ell_+, \ell_- + k_-, \boldsymbol{\ell}_\perp)$

(b)

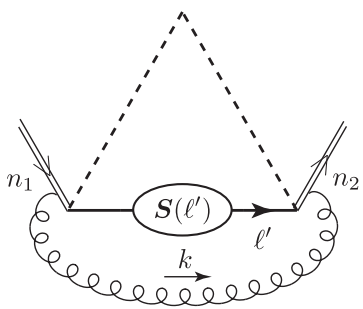

$\ell' = (\ell_+ - k_+, \ell_- - k_-, \boldsymbol{\ell}_\perp)$

(a)

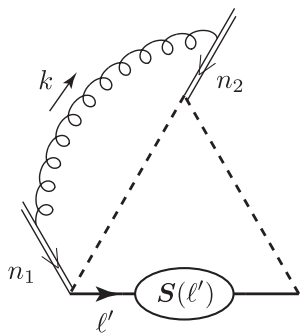

$\ell' = (\ell_+ - k_+, \ell_-, \boldsymbol{\ell}_\perp)$

(b)

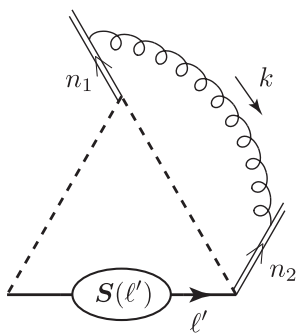

$\ell' = (\ell_+, \ell_- - k_-, \boldsymbol{\ell}_\perp)$

(c)

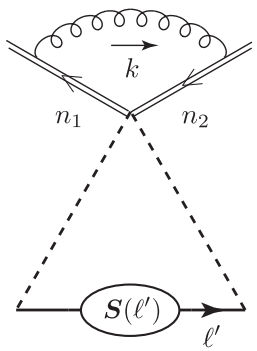

$\ell' = (\ell_+, \ell_-, \boldsymbol{\ell}_\perp)$

(d)

Diagram A

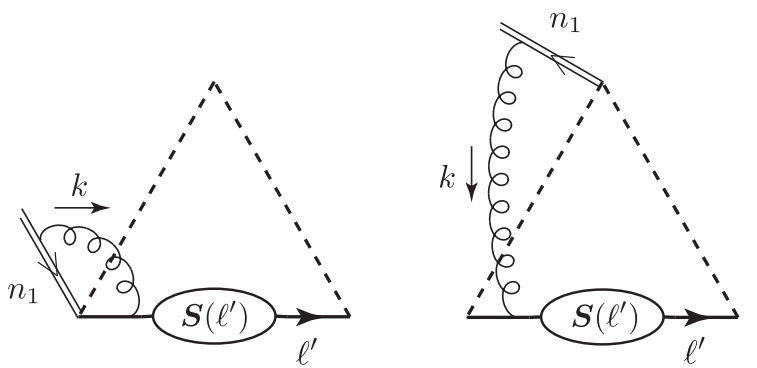

The non-local terms come from diagram (b).

$$
\begin{aligned}
\boldsymbol{S}_{(A)}(\ell_+,\ell_-) \;=\;& ig_s^2 C_F \left(\frac{\mu^2 e^{\gamma_E}}{4\pi}\right)^{\epsilon} \int_{\boldsymbol{\ell}_\perp} \int \frac{dk_+ dk_- d^{D-2}k_\perp}{(2\pi)^D} \frac{1}{(-k_+ + i\varepsilon)(k^2 + i\varepsilon)} \\
&\times \Bigg\{ - \frac{\boldsymbol{S}(\ell_+,\ell_-,\ell_\perp) \frac{\not{n}_1}{2} \left[\frac{\not{n}_2}{2}(\ell_+ - k_+) + \not{\ell}_\perp - \not{k}_\perp + m_b\right]}{(\ell_+ - k_+)(\ell_- - k_-) - (\boldsymbol{\ell}_\perp - \boldsymbol{k}_\perp)^2 - m_b^2 + i\varepsilon} \\
&\quad + \frac{\boldsymbol{S}(\ell_+ + k_+,\ell_-,\ell_\perp) \frac{\not{n}_1}{2} (\frac{\not{n}_2}{2}\ell_+ + \not{\ell}_\perp - \not{k}_\perp + m_b)}{\ell_+(\ell_- - k_-) - (\boldsymbol{\ell}_\perp - \boldsymbol{k}_\perp)^2 - m_b^2 + i\varepsilon} \Bigg\}. \qquad (17)
\end{aligned}
$$

k_- contour integration

Assuming $\ell_+ > 0$, $\ell_- < 0$ and completing the k_- contour integration by picking up the pole $k_- = \frac{k_\perp^2}{k_+} - i\varepsilon$

$$
\begin{aligned}
\boldsymbol{S}_{(A)}(\ell_+,\ell_-) \quad = \quad & -2\alpha_s C_F \left(\frac{\mu^2 e^{\gamma_E}}{4\pi}\right)^{\epsilon} \int_{\boldsymbol{\ell}_\perp} \int \frac{d^{D-2}k_\perp}{(2\pi)^{D-2}} \int_0^\infty \frac{dk_+}{k_+^2} \\
& \times \Bigg\{ - \frac{\theta(\ell_+ - k_+)\boldsymbol{S}(\ell_+,\ell_-)\frac{\not{n}_1}{2}\left[\frac{\not{n}_2}{2}(\ell_+ - k_+) + \not{\ell}_\perp - \not{k}_\perp + m_b\right]}{(\ell_+ - k_+)\ell_- - \frac{\ell_+ - k_+}{k_+}\boldsymbol{k}_\perp^2 - (\boldsymbol{\ell}_\perp - \boldsymbol{k}_\perp)^2 - m_b^2 + i\varepsilon} \\
& + \frac{\boldsymbol{S}(\ell_+ + k_+,\ell_-,\ell_\perp)\frac{\not{n}_1}{2}(\frac{\not{n}_2}{2}\ell_+ + \not{\ell}_\perp - \not{k}_\perp + m_b)}{\ell_+\ell_- - \frac{\ell_+}{k_+}\boldsymbol{k}_\perp^2 - (\boldsymbol{\ell}_\perp - \boldsymbol{k}_\perp)^2 - m_b^2 + i\varepsilon} \Bigg\}. \qquad (18)
\end{aligned}
$$

Extract UV divergences

After shifting $k_\perp$

$$
\begin{aligned}
\boldsymbol{S}_{(A)}(\ell_+,\ell_-) \;=\; & 2\alpha_s C_F \left(\frac{\mu^2 e^{\gamma_E}}{4\pi}\right)^{\epsilon} \int_{\boldsymbol{\ell}_\perp} \int \frac{d^{D-2}k_\perp}{(2\pi)^{D-2}} \int_0^\infty \frac{dk_+}{k_+} \\
& \times \Bigg\{ -\frac{\theta(\ell_+-k_+)}{\ell_+} \frac{\boldsymbol{S}(\ell_+,\ell_-)\frac{\not{n}_1}{2}\left[\frac{\not{n}_2}{2}(\ell_+-k_+)+\boldsymbol{\ell}\!\!\!/_\perp \frac{\ell_+-k_+}{\ell_+}+m_b\right]}{\boldsymbol{k}_\perp^2 - \frac{k_+}{\ell_+}\left(\ell^2-m_b^2-\ell_- k_+ + \frac{k_+}{\ell_+}\boldsymbol{\ell}_\perp^2\right)-i\varepsilon} \\
& + \frac{1}{\ell_++k_+} \frac{\boldsymbol{S}(\ell_++k_+,\ell_-,\ell_\perp)\frac{\not{n}_1}{2}\left(\frac{\not{n}_2}{2}\ell_+ + \boldsymbol{\ell}\!\!\!/_\perp \frac{\ell_+}{\ell_++k_+}+m_b\right)}{\boldsymbol{k}_\perp^2 - \frac{k_+\ell_+\left(\ell^2-m_b^2\right)+k_+^2\left(\ell_+\ell_- - m_b^2\right)}{\left(\ell_++k_+\right)^2}-i\varepsilon} \Bigg\}.
\end{aligned}
\tag{19}
$$

Extract the UV divergences from $k_\perp$ integration:

$$
\begin{aligned}
\boldsymbol{S}^{\text{UV}}_{(A)}(\ell_+,\ell_-) \;=\; & \frac{\alpha_s C_F}{2\pi}\frac{1}{\epsilon_{\text{UV}}} \int_{\boldsymbol{\ell}_\perp} \int_0^\infty \frac{dk_+}{k_+} \\
& \times \Bigg\{ -\boldsymbol{S}(\ell_+,\ell_-,\ell_\perp)\frac{\not{n}_1}{2}\frac{\theta(\ell_+-k_+)\left[\frac{\not{n}_2}{2}(\ell_+-k_+)+\boldsymbol{\ell}\!\!\!/_\perp\frac{\ell_+-k_+}{\ell_+}+m_b\right]}{\ell_+} \\
& + \boldsymbol{S}(\ell_++k_+,\ell_-,\ell_\perp)\frac{\not{n}_1}{2}\frac{\left(\frac{\not{n}_2}{2}\ell_+ + \boldsymbol{\ell}\!\!\!/_\perp\frac{\ell_+}{\ell_++k_+}+m_b\right)}{\ell_++k_+} \Bigg\}.
\end{aligned}
\tag{20}
$$

UV divergence of diagram A

The change of variables $k_+ = x\ell_+$ leads to

$$\begin{aligned} \boldsymbol{S}^{\rm UV}_{(A)}(\ell_+,\ell_-) &= \frac{\alpha_s C_F}{2\pi}\frac{1}{\epsilon_{\rm UV}}\int_{\boldsymbol{\ell}_\perp}\left\{\boldsymbol{S}(\ell_+,\ell_-,\ell_\perp)\frac{\not{n}_1}{2}\left(\frac{\not{n}_2}{2}+\frac{\not{\ell}_\perp}{\ell_+}\right)\right. \\ &+\int_0^\infty dx\left[\frac{\boldsymbol{S}(\ell_+(1+x),\ell_-,\ell_\perp)}{x(1+x)}\frac{\not{n}_1}{2}\left(\frac{\not{n}_2}{2}+\frac{\not{\ell}_\perp}{\ell_+}\frac{1}{1+x}+\frac{m_b}{\ell_+}\right)\right. \\ &\left.\left.-\frac{\theta(1-x)\boldsymbol{S}(\ell_+,\ell_-,\ell_\perp)}{x}\frac{\not{n}_1}{2}\left(\frac{\not{n}_2}{2}+\frac{\not{\ell}_\perp}{\ell_+}+\frac{m_b}{\ell_+}\right)\right]\right\}. \end{aligned} \tag{21}$$

Transformations $\frac{x}{1-x} \to u \to x$ for $\boldsymbol{S}(\ell_+,\ell_-,\ell_\perp)$ terms

$$\begin{aligned} &\boldsymbol{S}^{\rm UV}_{(A)}(\ell_+,\ell_-) \\ =\ &\frac{\alpha_s C_F}{2\pi}\frac{1}{\epsilon_{\rm UV}}\int_{\boldsymbol{\ell}_\perp}\left[\boldsymbol{S}(\ell_+,\ell_-,\ell_\perp)\left(1-\frac{\not{n}_2\not{n}_1}{4}+\frac{n_2\cdot\ell}{\omega}\frac{\not{n}_1\not{\ell}_\perp}{2}\right)\right. \\ &+\int_0^\infty dx\left\{\frac{\boldsymbol{S}(\ell_+(1+x),\ell_-,\ell_\perp)}{x(1+x)}\left[1-\frac{\not{n}_2\not{n}_1}{4}+\frac{n_2\cdot\ell}{(1+x)\omega}\frac{\not{n}_1\not{\ell}_\perp}{2}+\frac{m_b(n_2\cdot\ell)}{\omega}\frac{\not{n}_1}{2}\right]\right. \\ &\left.\left.-\frac{\boldsymbol{S}(\ell_+,\ell_-,\ell_\perp)}{x(1+x)}\left[1-\frac{\not{n}_2\not{n}_1}{4}+\frac{n_2\cdot\ell}{\omega}\frac{\not{n}_1\not{\ell}_\perp}{2}+\frac{m_b(n_2\cdot\ell)}{\omega}\frac{\not{n}_1}{2}\right]\right\}\right]. \end{aligned} \tag{22}$$

UV divergence of diagram A′

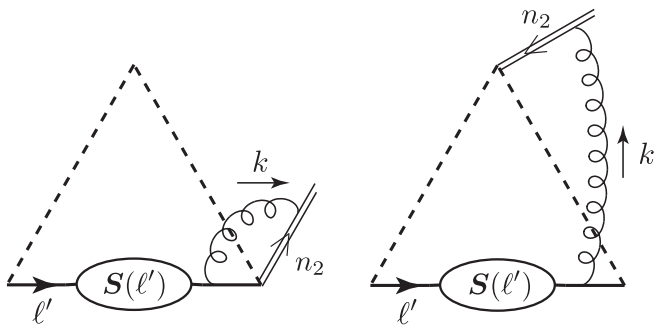

The non-local terms come from diagram (b).

$$
\begin{aligned}
& \boldsymbol{S}^{\text{UV}}_{(A')}(\ell_+, \ell_-) \\
= \quad & \frac{\alpha_s C_F}{2\pi} \frac{1}{\epsilon_{\text{UV}}} \int_{\boldsymbol{\ell}_\perp} \left[\left(1 - \frac{\not{n}_2 \not{n}_1}{4} + \frac{n_1 \cdot \ell}{\omega} \frac{\not{\ell}_\perp \not{n}_2}{2} \right) \boldsymbol{S}(\ell_+, \ell_-, \boldsymbol{\ell}_\perp) \right. \\
& + \int_0^\infty dx \left\{ \left[1 - \frac{\not{n}_2 \not{n}_1}{4} + \frac{n_1 \cdot \ell}{(1+x)\omega} \frac{\not{\ell}_\perp \not{n}_2}{2} + \frac{m_b (n_1 \cdot \ell)}{\omega} \frac{\not{n}_2}{2} \right] \frac{\boldsymbol{S}(\ell_+, (1+x)\ell_-, \boldsymbol{\ell}_\perp)}{x(1+x)} \right. \\
& \left. \left. - \left[1 - \frac{\not{n}_2 \not{n}_1}{4} + \frac{n_1 \cdot \ell}{\omega} \frac{\not{\ell}_\perp \not{n}_2}{2} + \frac{m_b (n_1 \cdot \ell)}{\omega} \frac{\not{n}_2}{2} \right] \frac{\boldsymbol{S}(\ell_+, \ell_-, \boldsymbol{\ell}_\perp)}{x(1+x)} \right\} \right].
\end{aligned}
\tag{23}
$$

Diagram B

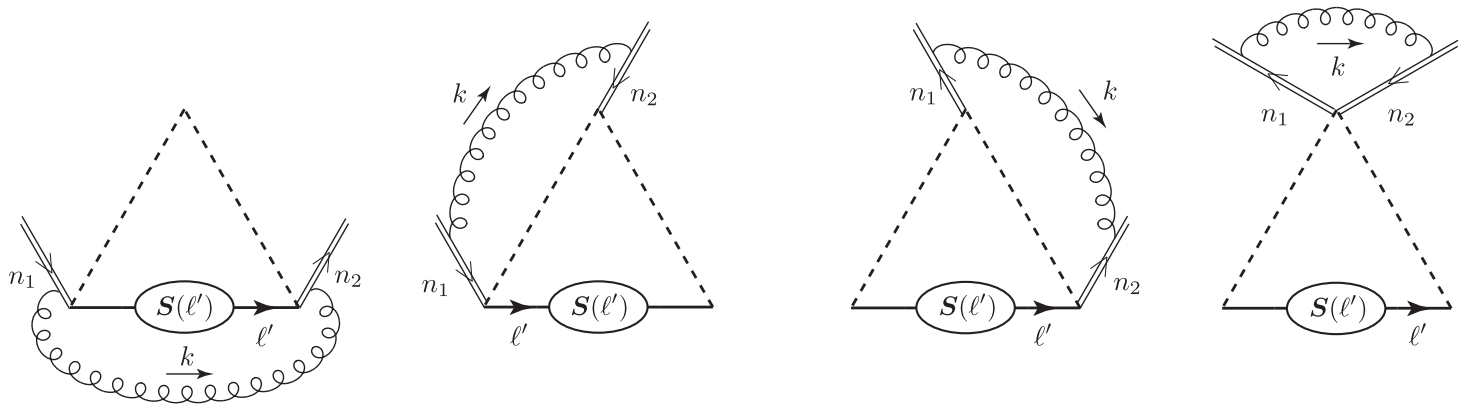

$\ell' = (\ell_+ - k_+, \ell_- - k_-, \boldsymbol{\ell}_\perp)$ (a)

$\ell' = (\ell_+ - k_+, \ell_-, \boldsymbol{\ell}_\perp)$ (b)

$\ell' = (\ell_+, \ell_- - k_-, \boldsymbol{\ell}_\perp)$ (c)

$\ell' = (\ell_+, \ell_-, \boldsymbol{\ell}_\perp)$ (d)

The non-local terms come from diagram (a, b, c).

$$\begin{aligned} \boldsymbol{S}_{(B)}(\ell_+, \ell_-) \quad = \quad & i g_s^2 C_F \left(\frac{\mu^2 e^{\gamma_E}}{4\pi}\right)^{\epsilon} \int \frac{dk_+ dk_- d^{D-2} k_\perp}{(2\pi)^D} \frac{1}{(-k_+ + i\varepsilon)(k_- + i\varepsilon)(k^2 + i\varepsilon)} \\ & \times \big[\boldsymbol{S}(\ell_+ - k_+, \ell_- - k_-) - \boldsymbol{S}(\ell_+ - k_+, \ell_-) \\ & - \boldsymbol{S}(\ell_+, \ell_- - k_-) + \boldsymbol{S}(\ell_+, \ell_-)\big]. \end{aligned} \tag{24}$$

k_- contour integration

Completing k_- contour integration gives

$$\begin{aligned}\boldsymbol{S}_{(B)}(\ell_+,\ell_-) &= -2\alpha_s C_F\left(\frac{\mu^2 e^{\gamma_E}}{4\pi}\right)^{\epsilon}\int_{-\infty}^{0}\frac{dk_+}{(-k_+)}\int\frac{d^{D-2}k_\perp}{(2\pi)^{D-2}}\frac{1}{\boldsymbol{k}_\perp^2}\\ &\times\Big[\theta(\ell_+-k_+)\boldsymbol{S}(\ell_+-k_+,\ell_-)+\theta(k_+-\ell_+)\boldsymbol{S}(\ell_+-k_+,\ell_--\tfrac{\boldsymbol{k}_\perp^2}{k_+})\\ &-\boldsymbol{S}(\ell_+-k_+,\ell_-)-\boldsymbol{S}(\ell_+,\ell_--\tfrac{\boldsymbol{k}_\perp^2}{k_+})+\boldsymbol{S}(\ell_+,\ell_-)\Big].\end{aligned}\tag{25}$$

Making the change of variables $\boldsymbol{k}_\perp^2=xk_+\ell_-$ and splitting the k_+ integration region $[-\infty,0]$ into $[-\infty,\ell_+]$ and $[\ell_+,0]$, we obtain

$$\begin{aligned}\boldsymbol{S}_{(B)}(\ell_+,\ell_-) &= \frac{\alpha_s C_F}{2\pi}\frac{\left(\mu^2 e^{\gamma_E}\right)^{\epsilon}}{\Gamma(1-\epsilon)}(\ell_-)^{-\epsilon}\int_{-\infty}^{0}dx\,\frac{1}{(-x)^{1+\epsilon}}\\ &\times\Big\{\int_{\ell_+}^{0}\frac{dk_+}{(-k_+)^{1+\epsilon}}\Big[\boldsymbol{S}(\ell_+-k_+,\ell_-)-\boldsymbol{S}(\ell_+-k_+,\ell_-(1-x))\\ &\qquad+\boldsymbol{S}(\ell_+,\ell_-(1-x))-\boldsymbol{S}(\ell_+,\ell_-)\Big]\\ &+\int_{-\infty}^{\ell_+}\frac{dk_+}{(-k_+)^{1+\epsilon}}\Big[\boldsymbol{S}(\ell_+,\ell_-(1-x))-\boldsymbol{S}(\ell_+,\ell_-)\Big]\Big\}.\end{aligned}\tag{26}$$

The UV divergences come from x integrations and k_+ integrations.

UV divergence of diagram B

Extracting the UV divergences and, for the finite k_+ integral, after extracting UV divergences from x integration, we set $k_+ = x\ell_+$:

$$\begin{aligned} & \boldsymbol{S}^{\rm UV}_{(B)}(\ell_+,\ell_-) \\ = \quad & \frac{\alpha_s C_F}{2\pi}\frac{1}{\epsilon_{\rm UV}}\left\{-\left[\frac{1}{\epsilon_{\rm UV}}+\log\left(\frac{\mu^2}{-\omega-i\varepsilon}\right)\right]\boldsymbol{S}(\ell_+,\ell_-)-\int_{-\infty}^{-1}dx\,\frac{\boldsymbol{S}(\ell_+,\ell_-(1-x))}{x}\right. \\ & \left.+\int_0^1 dx\,\frac{\boldsymbol{S}(\ell_+(1-x),\ell_-)-\boldsymbol{S}(\ell_+,\ell_-)}{x}-\int_{-1}^0 dx\,\frac{\boldsymbol{S}(\ell_+,\ell_-(1-x))-\boldsymbol{S}(\ell_+,\ell_-)}{x}\right\}. \end{aligned} \tag{27}$$

We re-write the negative x integration as

$$\begin{aligned} & -\int_{-\infty}^{-1}\frac{dx}{x}\boldsymbol{S}(\ell_+,\ell_-(1-x))-\int_{-1}^{0}\frac{dx}{x}\left[\boldsymbol{S}(\ell_+,\ell_-(1-x))-\boldsymbol{S}(\ell_+,\ell_-)\right] \\ = \quad & \lim_{\delta\to 0}\left[-\int_{-\infty}^{-\delta}\frac{dx}{x}\boldsymbol{S}(\ell_+,\ell_-(1-x))-\int_{-1}^{-\delta}\frac{dx}{x}\boldsymbol{S}(\ell_+,\ell_-)\right] \end{aligned} \tag{28}$$

The contribution of the semicircle at infinity vanishes, and the contribution of the small semicircle is $\pm i\pi S(\omega)$. Then we split the integration region $[0,+\infty]$ into $[0,1]$ and $[1,+\infty]$.

UV divergences of diagram B and C

UV divergence of diagram B

$$\begin{aligned} \boldsymbol{S}^{\rm UV}_{(B)}(\ell_+,\ell_-) &= \frac{\alpha_s C_F}{2\pi}\frac{1}{\epsilon_{\rm UV}}\left\{-\left[\frac{1}{\epsilon_{\rm UV}}+\log\left(\frac{\mu^2}{\omega+i\varepsilon}\right)\right]\boldsymbol{S}(\ell_+,\ell_-)\right. \\ &\quad +\int_0^1 dx\,\frac{\boldsymbol{S}(\ell_+(1-x),\ell_-)+\boldsymbol{S}(\ell_+,\ell_-(1-x))-2\boldsymbol{S}(\ell_+,\ell_-)}{x} \\ &\quad \left.+\int_1^\infty dx\,\frac{\boldsymbol{S}(\ell_+,\ell_-(1-x))}{x}\right\}. \end{aligned} \tag{29}$$

UV divergence of the soft quark self-energy diagram (after renormalization of quark mass):

$$\boldsymbol{S}^{\rm UV}_{(C)}(\ell_+,\ell_-) = -\frac{\alpha_s C_F}{4\pi}\frac{1}{\epsilon_{\rm UV}}\boldsymbol{S}(\ell_+,\ell_-), \tag{30}$$

which is the soft-quark wave-function renormalization.

Total UV divergence at α_s order

$$
\begin{aligned}
\boldsymbol{S}^{\rm UV}(\ell_+,\ell_-) &= \boldsymbol{S}^{\rm UV}_{(A)}(\ell_+,\ell_-)+\boldsymbol{S}^{\rm UV}_{(A')}(\ell_+,\ell_-)+\boldsymbol{S}^{\rm UV}_{(B)}(\ell_+,\ell_-)+\boldsymbol{S}^{\rm UV}_{(C)}(\ell_+,\ell_-)\\
&= \frac{\alpha_s C_F}{2\pi}\frac{1}{\epsilon_{\rm UV}}\int_{\boldsymbol{\ell}_\perp}\Bigg[\boldsymbol{S}(\ell_+,\ell_-,\ell_\perp)\left(1-\frac{\not{n}_2\not{n}_1}{4}+\frac{n_2\cdot\ell}{\omega}\frac{\not{n}_1\not{\ell}_\perp}{2}\right)\\
&\quad+\int_0^\infty dx\Bigg\{\frac{\boldsymbol{S}(\ell_+(1+x),\ell_-,\ell_\perp)}{x(1+x)}\left[1-\frac{\not{n}_2\not{n}_1}{4}+\frac{n_2\cdot\ell}{(1+x)\omega}\frac{\not{n}_1\not{\ell}_\perp}{2}+\frac{m_b(n_2\cdot\ell)}{\omega}\frac{\not{n}_1}{2}\right]\\
&\quad-\frac{\boldsymbol{S}(\ell_+,\ell_-,\ell_\perp)}{x(1+x)}\left[1-\frac{\not{n}_2\not{n}_1}{4}+\frac{n_2\cdot\ell}{\omega}\frac{\not{n}_1\not{\ell}_\perp}{2}+\frac{m_b(n_2\cdot\ell)}{\omega}\frac{\not{n}_1}{2}\right]\Bigg\}\Bigg]\\
&\quad+\frac{\alpha_s C_F}{2\pi}\frac{1}{\epsilon_{\rm UV}}\int_{\boldsymbol{\ell}_\perp}\Bigg[\left(1-\frac{\not{n}_2\not{n}_1}{4}+\frac{n_1\cdot\ell}{\omega}\frac{\not{\ell}_\perp\not{n}_2}{2}\right)\boldsymbol{S}(\ell_+,\ell_-,\ell_\perp)\\
&\quad+\int_0^\infty dx\Bigg\{\left[1-\frac{\not{n}_2\not{n}_1}{4}+\frac{n_1\cdot\ell}{(1+x)\omega}\frac{\not{\ell}_\perp\not{n}_2}{2}+\frac{m_b(n_1\cdot\ell)}{\omega}\frac{\not{n}_2}{2}\right]\frac{\boldsymbol{S}(\ell_+,(1+x)\ell_-,\ell_\perp)}{x(1+x)}\\
&\quad-\left[1-\frac{\not{n}_2\not{n}_1}{4}+\frac{n_1\cdot\ell}{\omega}\frac{\not{\ell}_\perp\not{n}_2}{2}+\frac{m_b(n_1\cdot\ell)}{\omega}\frac{\not{n}_2}{2}\right]\frac{\boldsymbol{S}(\ell_+,\ell_-,\ell_\perp)}{x(1+x)}\Bigg\}\Bigg]\\
&\quad+\frac{\alpha_s C_F}{2\pi}\frac{1}{\epsilon_{\rm UV}}\Bigg\{-\left[\frac{1}{\epsilon_{\rm UV}}+\log\left(\frac{\mu^2}{\omega}\right)\right]\boldsymbol{S}(\ell_+,\ell_-)+\int_1^\infty dx\,\frac{\boldsymbol{S}(\ell_+,\ell_-(1-x))}{x}\\
&\quad+\int_0^1 dx\,\frac{\boldsymbol{S}(\ell_+(1-x),\ell_-)+\boldsymbol{S}(\ell_+,\ell_-(1-x))-2\boldsymbol{S}(\ell_+,\ell_-)}{x}\Bigg\}\\
&\quad-\frac{\alpha_s C_F}{4\pi}\frac{1}{\epsilon_{\rm UV}}\int_{\boldsymbol{\ell}_\perp}\boldsymbol{S}(\ell_+,\ell_-,\ell_\perp).
\end{aligned}
\tag{31}
$$

Z_S at α_s order

Define several additional structure functions

$$\boldsymbol{S}_i(\omega) = \int_{\boldsymbol{\ell}_\perp} \boldsymbol{S}_i(\omega, \boldsymbol{\ell}_\perp^2) \frac{\boldsymbol{\ell}_\perp^2}{\omega}, \quad \text{for } i = 5, 6, 7, \text{ and } 8. \tag{32}$$

Make the following changes of integration variables: $\omega' = (1+x)\omega$ for $\boldsymbol{S}^{\rm UV}_{(A)}$ and $\boldsymbol{S}^{\rm UV}_{(A')}$, and $\omega' = (1-x)\omega$ for $\boldsymbol{S}^{\rm UV}_{(B)}$, then the renormalized structure functions can be expressed as

$$S_i^{\rm R}(\omega) = \sum_{j=1}^{8} \int_0^\infty d\omega' Z_S^{ij}(\omega, \omega'; \mu) S_j(\omega'), \quad \text{for } i = 1, 2, 3, \text{ and } 4, \tag{33}$$

where

$$Z_S^{ij}(\omega, \omega'; \mu) = \delta(\omega - \omega')\delta^{ij} + \frac{\alpha_s C_F}{4\pi} \frac{1}{\epsilon_{\rm UV}} \boldsymbol{M}_S^{ij}(\omega, \omega'; \mu), \tag{34}$$

$\boldsymbol{M}_S^{ij}(\omega,\omega';\mu)$

$$
\begin{aligned}
&\boldsymbol{M}_S(\omega,\omega';\mu)\\
&=\begin{pmatrix}
d-2a-2b-2c & 0 & 0 & 0 & 0 & 0 & 0 & 0\\
-\frac{m_b^2}{\omega}b & e & 0 & 0 & -(a+b) & 0 & 0 & 0\\
-\frac{m_b^2}{\omega}b & 0 & e & 0 & -(a+b) & 0 & 0 & 0\\
2(a+b) & -\frac{\omega'}{\omega}b & -\frac{\omega'}{\omega}b & d-2c & 0 & a+b & a+b & 0
\end{pmatrix},
\end{aligned}
\tag{35}
$$

with a, b, c, and d defined by

$$
\begin{aligned}
a &= 2\delta(\omega-\omega'),\quad b=2\left[\frac{\omega\theta(\omega'-\omega)}{\omega'(\omega'-\omega)}\right]_+,\quad c=2\left[\frac{\theta(\omega-\omega')}{\omega-\omega'}\right]_+,\\
d &= \left[\frac{2}{\epsilon_{\rm UV}}+2\log\left(\frac{\mu^2}{\omega}\right)+1\right]\delta(\omega-\omega'),\ e=d-a-\frac{\omega'}{\omega}b-\frac{\omega'+\omega}{\omega}c.
\end{aligned}
\tag{36}
$$

Here, the plus distribution is defined by

$$
\int_0^\infty d\omega'\,\frac{f(\omega')}{[g(\omega')]_+}=\int_0^\infty d\omega'\,\frac{f(\omega')-f(\omega)}{g(\omega')}.
\tag{37}
$$

Cannot solve the corresponding evolution equation in closed form because infinitely many new structure functions with different $\ell_\perp$ weights appear.

Z_S at α_s order for $H \to \gamma\gamma$ case

For the case of $H \to \gamma\gamma$ through b-quark loop, the soft function is sandwiched between $\not{n}_2$ and $\not{n}_1$, which means only the structure function $S_1(\omega)$ survives and does not involve mixing between structure functions

$$\begin{aligned} Z_S^{11} &= \delta(\omega'-\omega) + \frac{\alpha_s C_F}{4\pi}\frac{1}{\epsilon_{\rm UV}}(d-2a-2b-2c) \\ &= \delta(\omega'-\omega) + \frac{\alpha_s C_F}{4\pi}\frac{1}{\epsilon_{\rm UV}}\left\{\left[\frac{2}{\epsilon_{\rm UV}} + 2\log\left(\frac{\mu^2}{\omega}\right) - 3\right]\delta(\omega'-\omega)\right. \\ &\qquad \left. -4\omega\left[\frac{\theta(\omega'-\omega)}{\omega'(\omega'-\omega)} + \frac{\theta(\omega-\omega')}{\omega(\omega-\omega')}\right]_+\right\}. \end{aligned} \tag{38}$$

Confirms the conjecture in : Z. L. Liu, B. Mecaj, M. Neubert, X. Wang and S. Fleming, JHEP **07**, 104 (2020) at α_s order.

Radiative jet function

The radiative jet function:

$$\bar{J}(\bar{n}\cdot p, p^2) \equiv i\int d^D x\, e^{i\frac{\ell_+ x_-}{2}} \langle\gamma(k_1)|T\left(W_n^\dagger i\not{D}_n^\perp \xi_n\right)^a(x)\left(\bar{\xi}_n W_n\right)^b(0)|0\rangle. \tag{39}$$

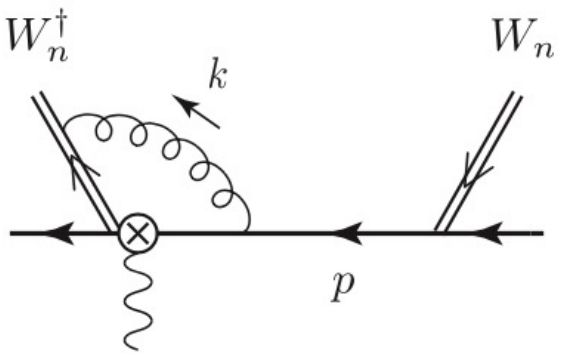

Figure: One of the radiative jet function Feynman diagrams at α_s order.

- W_n is collinear Wilson line.

Factor the soft contributions from $\bar{J}$

- Use the soft approximation and graphical Ward identities to factor the soft contributions (zero-bin subtractions) from the radiative jet function.
- S_n is soft Wilson line and W_n gives soft Wilson line $S_{\bar{n}}$ in the soft limit.
- p is the momentum that enters the radiative jet function along the quark line.

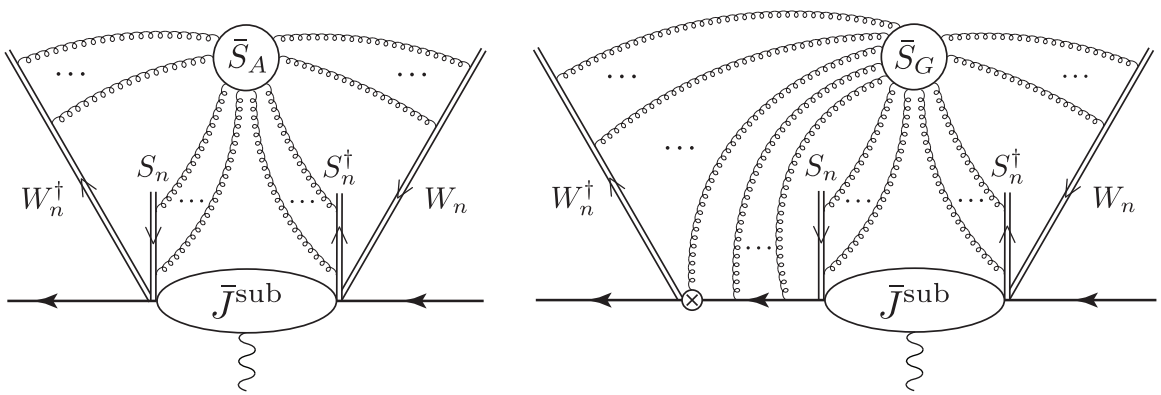

Figure: Diagrammatic representation of the extraction of the soft contributions from $\bar{J}$. $\bar{S}_A$ connects to Wilson lines only, $\bar{S}_G$ connects to Wilson lines and soft quark.

Soft subtraction and subtracted radiative jet function

Soft subtraction/Zero-bin subtraction:

$$\bar{S}(k_+) = \bar{S}_A(k_+) + \bar{S}_G(k_+), \tag{40}$$

where

$$\begin{aligned}
\bar{S}_A(k_+) &= \frac{p_+}{2\pi}\int\frac{dx_-}{2}\,e^{i\frac{k_+x_-}{2}}\langle 0|T(S_{\bar{n}}^{a\dagger}S_n^b)(x_-)(S_n^{b\dagger}S_{\bar{n}}^a)(0)|0\rangle,\\
\bar{S}_G(k_+) &= \frac{ip_+}{2\pi}\int d^Dy\int\frac{dx_-}{2}\,e^{i\frac{p_+y_-}{2}}\,e^{i\frac{(k_+-p_+)x_-}{2}}\\
&\quad\times\langle 0|T(S_{\bar{n}}^{a\dagger}P_n i\not{D}_s^{\perp}\psi_{n,s})(y)(S_n^b\bar{\psi}_{n,s}P_n)(x_-)(S_n^{b\dagger}S_{\bar{n}}^a)(0)|0\rangle
\end{aligned} \tag{41}$$

Then the radiative jet function can be expressed as convolution over the plus component of momentum:

$$\bar{J}(p_-p_+) = \int\frac{dk_+}{p_+}\bar{S}(k_+)\bar{J}^{\rm sub}\left[p_-(p_+-k_+)\right] \equiv \bar{S}\otimes\bar{J}^{\rm sub}. \tag{42}$$

Consequently,

$$\bar{J}^{\rm sub} = \bar{S}^{-1}\otimes\bar{J}. \tag{43}$$

- In renormalizing $\bar{J}^{\rm sub}$, we obtain renormalizations from both $\bar{S}^{-1}$ and $\bar{J}$.

Renormalization formula

Renormalization formula

$$\bar{J}_R^{\rm sub}(p^2;\mu) = \int dx\, Z_{\bar{J}\,{\rm sub}}[(1-x)p_+, p^2;\mu]\bar{J}^{\rm sub}(xp^2), \tag{44}$$

where

$$Z_{\bar{J}\,{\rm sub}}[(1-x)p_+, p^2;\mu] = Z_{\bar{J}}(p^2;\mu)Z_{\bar{S}}^{-1}[(1-x)p_+;\mu]. \tag{45}$$

Note that the renormalization of the un-subtracted jet function is local and the soft subtraction renormalization is non-local!

At α_s order (one-loop level):

$$\bar{J}_R^{\rm sub} = [\mathbf{1} + \alpha_s Z^{(1)}_{\bar{J}{\rm sub}} + O(\alpha_s^2)] \otimes \bar{J}^{\rm sub}, \tag{46}$$

where

$$Z^{(1)}_{\bar{J}\,{\rm sub}} = Z^{(1)}_{\bar{J}}\delta(1-x) - Z^{(1)}_{\bar{S}}. \tag{47}$$

One-loop radiative jet function Feynman diagrams

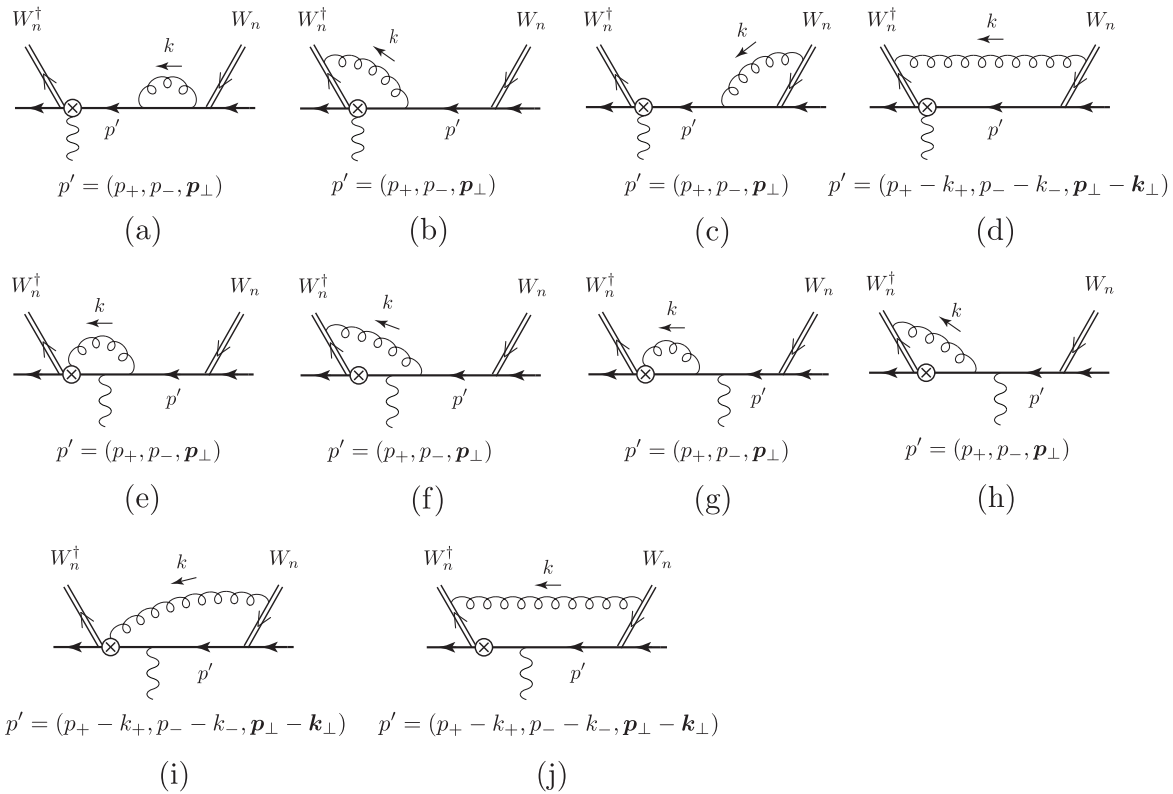

Figure: Feynman diagrams that may contribute to the renormalization of the radiative jet function $\bar{J}$ in order α_s.

Diagrams (d), (i), (j) do not contribute to UV divergences.
The renormalization of un-subtracted jet function is local!

One-loop soft subtraction function Feynman diagrams

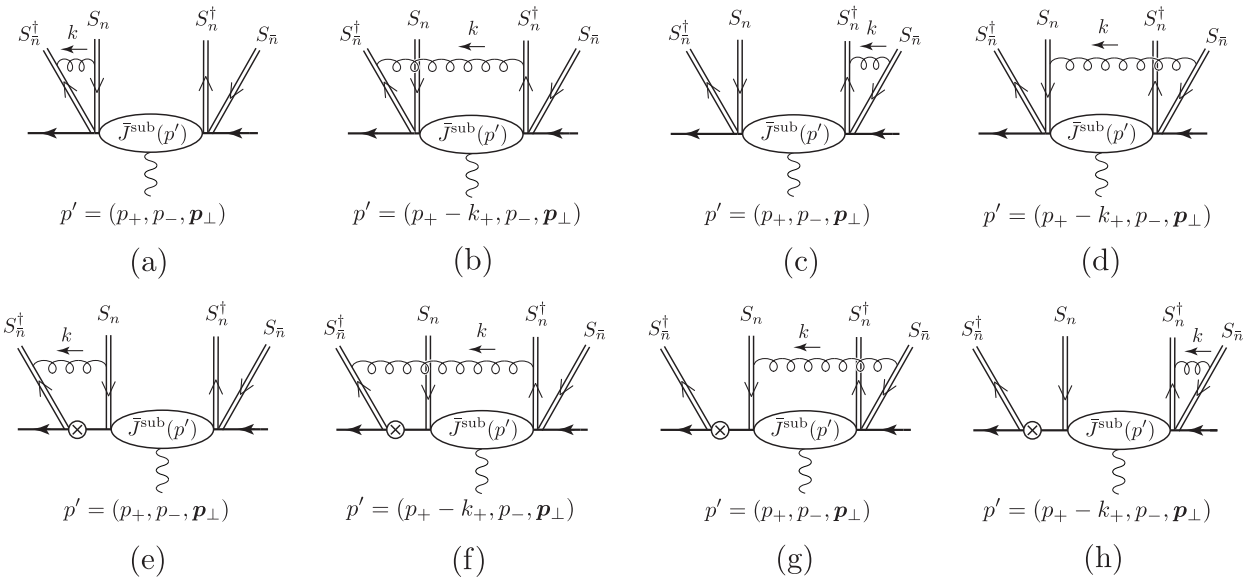

Figure: Feynman diagrams that contribute to the renormalization of the soft subtraction function $\bar{S}$ in order α_s. Diagrams (b,d,f,h) lead to non-local renormalization!

- Note: The renormalization of radiative jet function and soft subtraction involve rapidity divergences separately. However, once we combine them together, the rapidity divergences cancel.

Results

Up to order α_s,

$$Z_J^{\rm sub} = \left[1 + \frac{\alpha_s C_F}{4\pi}\left(-\frac{2}{\epsilon^2} - \frac{2}{\epsilon}\ln\frac{\mu^2}{-p^2 - i\varepsilon}\right)\right]\delta(1-x) + \frac{\alpha_s C_F}{2\pi\epsilon}\Gamma(1,x), \qquad (48)$$

where

$$\Gamma(1,x) = \left[\frac{\theta(1-x)}{1-x} + \frac{\theta(x-1)}{x(x-1)}\right]_+ . \qquad (49)$$

- $\Gamma(1,x)$ is the non-local part and comes entirely from the soft subtraction.
- Our result is in agreement with the one-loop result that had been inferred from the factorization theorem for $B \to \gamma\ell^-\nu$ [Bosch, Hill, Lange, Neubert (2003)].
- However, the renormalization kernel inferred from the factorization theorem for $B \to \gamma\ell^-\nu$ was in ascribed to $\bar{J}$, rather than to $\bar{J}^{\rm sub}$.

Summary

- The unorthodox momentum routing of the soft-quark function leads to non-local contributions in the renormalization, which makes the renormalization non-trivial.
- We have explained how to renormalize the soft-quark function and confirmed the conjecture given in the literature at α_s order.
- To avoid double counting of soft contributions, the factorization theorems should be expressed in terms of a subtracted jet function.
- We showed that the soft subtractions can be factored from the radiative jet function and that the resulting soft-subtraction function gives rise to a nonlocal renormalization of the subtracted radiative jet function.
- This is the first known instance of nonlocal renormalization from zero-bin subtractions.
- Our one-loop result agrees with the evolution kernel deduced by using the factorization theorem for $B \to \gamma \ell^- \nu$. [Bosch, Hill, Lange, Neubert(2003). Wrongly attributed to the radiative jet function, rather than to the subtracted radiative jet function.]